Ultra Fast and Parsimonious Materials Screening for Polymer Solar Cells Using Differentially Pumped Slot-Die Coating

Jan Alstrup, Mikkel Jørgensen, Andrew J. Medford, and Frederik C. Krebs*

Risø National Laboratory for Sustainable Energy, Technical University of Denmark Frederiksborgvej 399, DK-4000 Roskilde, Denmark

ABSTRACT We present a technique that enables the probing of the entire parameter space for each parameter with good statistics through a simple roll-to-roll processing method where gradients of donor, acceptor, and solvent are applied by differentially pumped slot-die coating. We thus demonstrate how the optimum donor−acceptor ratio and device film thickness can be determined with improved accuracy by varying the composition in small steps. We give as an example P3HT-PCBM devices and vary the composition between P3HT and PCBM in steps of 0.5−1% giving 100−200 individual solar cells. The coating experiment itself takes less than 4−8 min and requires 15−30 mg each of donor and acceptor material. The optimum donor−acceptor composition of P3HT and PCBM was found to be a broad maximum centered on a 1:1 ratio. We demonstrate how the optimal thickness of the active layer can be found by the same method and materials usage by variation of the layer thickness in small steps of 1.5−4 nm. Contrary to expectation we did not find oscillatory variation of the device performance with device thickness because of optical interference. We ascribe this to the nature of the solar cell type explored in this example that employs nonreflective or semitransparent printed electrodes. We further found that very thick active layers on the order of 1 μm can be prepared without loss in performance and estimate the active layer thickness could easily approach 4−5 μm while maintaining photovoltaic properties.

KEYWORDS: slot-die coating • differential pumping • polymer solar cells • gradients • mixing • thickness

INTRODUCTION

Polymer solar cells (1) efficiently address the problem of a too high cost of materials and manufacturing that most other photovoltaic technologies suffer from. They rely on thin organic films that can be applied by fast roll-to-roll processing methods (2). It has been demonstrated that polymer solar cells can yield significant performance, a reasonable stability and low process cost (3). There is, however, still a significant amount of fundamental research and technical development needed before polymer solar cells can be anticipated to compete with, e.g., silicon solar cells. The reasons for this are the exceptionally complex makeup of polymer solar cells and the difficulty by which the correctly optimized device is reached. Polymer solar cells have been moving rapidly toward large scale manufacture and demonstration but there are still massive scientific challenges to overcome. The optimization of polymer solar cell performance and evaluation of new materials requires schemes that probe several processing dimensions such as device layer thicknesses, processing solvents, and donor−acceptor ratios. The only available procedure until now has been the sampling of discrete points in this complex parameter space by individual experiments. When investigating newly developed materials, this involves the preparation of many solutions and most commonly the films for the active layer are prepared by spin-coating, which implies a significant loss of material, and it has been shown several times that unintended variability is introduced making it impossible to identify all the sources of variation in experimental data. The careful optimization of, for instance, the layer thickness and the donor−acceptor ratio will thus easily require in excess of one hundred milligrams of material and in cases where many devices must be prepared for each parameter to get good statistics gram quantities are required. To illustrate how the scale of the problem juxtaposes with our capacity to sample the parameter space, we can consider a typical polymer solar cell and the number of ways in which it can be constituted. The typical solar cell comprises a substrate and barriers (5 typical choices), a transparent electrode (5 typical choices), a hole transport layer (5 typical choices), the active donor material (>100 typical choices), the active acceptor material (5 typical choices), an electron transport layer (5 typical choices), and a back electrode (10 typical choices). The values in brackets represent the number of typical materials choices available when composing a random polymer solar cell. The parameter space and typical multilayer structure is illustrated in Figure 1 and presents just one example of a polymer solar cell. By random sampling, we can estimate the total number of material combinations that can be used to prepare polymer solar cells to be in the range of 1 million (based on this design and these materials). Once the device constitution in terms of materials has been chosen, the device has to be optimized with respect to the mode of preparation and at least in terms of thickness, but possibly also with respect to additives. If the individual layers in Figure 1 are taken in turn the difficulty in optimiza-

* Corresponding author. E-mail: frkr@risoe.dtu.dk.
Received for review June 9, 2010 and accepted September 13, 2010

DOI: 10.1021/am100505e

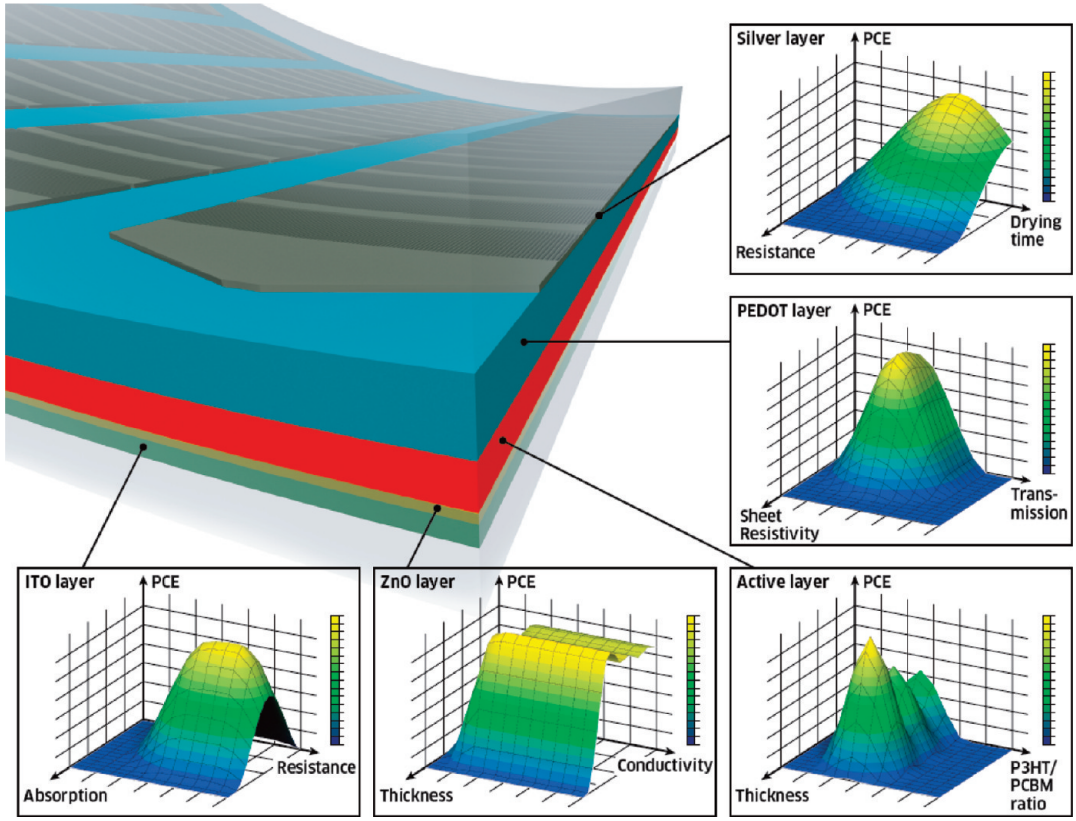

FIGURE 1. Simplified drawing of the layered structure in a typical OPV illustrating how each of the (in this case) 5 layers must be optimized with respect to several influential parameters. For each layer, it is illustrated how the performance might be optimized with respect to two typical parameters.

tion becomes evident. The substrate, which in this case is PET, can present problems of thermal stability such as shrinkage that during many heat−cool cycles may affect performance in a manner that is difficult to isolate in optimization experiments. The ITO layer is the first functional layer and although it is mostly purchased from a supplier and in many ways outside the control of the experimenter, the preparation and pretreatments may affect performance. It is sensitive to flexing and bending and its work function critically depends on the cleaning and patterning methods. The conductivity and the transmission of light through the ITO layer will thus have a major influence on the performance where the aim is to have a high conductivity while maintaining a high transmission. Because these parameters are counteracting the optimization of these two presents a maximum. The zinc oxide layer acts as a selective electron transport layer and needs to be as thin as possible while being transparent and hole blocking. When very thin, performance will be limited, and smaller thicknesses may present an optical interference effect. The active layer may present a more complex problem especially if it is of the most common bulk hetero junction type. This layer is often a mixture of a conjugated polymer as electron donor material (such as P3HT) and an electron acceptor material (such as 60PCBM) comprising a bulk hetero junction where the amount of each component can be varied. It is also very important to optimize the nanostructure using a number of techniques such as temperature (4) and/or solvent annealing (5). When using spin-coating to deposit this layer it has been found that the solvent used greatly influences the final film morphology. Recently additives such as 1,8-octanedithiole (6) or 1,8-diodooctane (7) have been introduced to improve performance to today's record level ~8 % (8). The thickness and the donor−acceptor ratio present an optimum as shown in Figure 1, which has a maximum performance at a particular ratio and reportedly also optical interference effects as a function of thickness. The PEDOT:PSS layer present a maximum at a particular thickness (and optical transmission during back illumination) and the silver layer present a dependence on the drying time and the resistivity. The resistance obtained depends critically on the drying time. With too short drying the resistivity is high and with too long drying the resistivity also becomes high. It is not straightforward to assess how many experiments would be necessary to thoroughly investigate all these parameters, but it is obvious that the parameter space is huge even after selecting the geometry and materials of the solar cell. To efficiently sample such a large parameter space, highly efficient methods are needed and the current approaches fall short of fulfilling this goal. In the typical experiment of optimizing, e.g., the donor−acceptor ratio, components have to be accurately weighed, mixed, dissolved, filtered, and spin-coated onto a laboriously cleaned substrate that may already include some of the layers in the solar cell stack.

This not only introduces many sources of error but also requires significant amounts of material and time. Once the materials are mixed in the required ratio, they cannot be

easily recovered, and unless all the material is used, excess material must be considered lost. In addition, the devices are typically prepared in batches with significant waiting times and the sources of error are many as pointed out by both Riede et al. (9) and Tromholt et al. (10). Both studies found that experimental variation beyond (human) control was automatically included in this approach despite careful examination of a considerable number of solar cells. This implies that even the most studied polymer solar cell based on P3HT and PCBM is unlikely to be fully characterized even when considering the standard laboratory device. Finally, once the particular device situation has been optimized using this methodology there is the additional problem of transferring the laboratory result to a setting that allows for industrial manufacture. This again may present an enormous effort in both time and materials.

It is clear that the currently available approach present some fundamental limitations and that the advancement of polymer solar cells would benefit greatly from a novel methodology that presents an increase in speed, accurate sampling of the parameter space, inherently fewer sources of experimental variation, less materials usage and an experimental form with greater proximity to a process capable of delivering polymer solar cells as a product. In this report, we present such a method that is simple in use.

EXPERIMENTAL SECTION

General Materials. Chlorobenzene was used as the solvent for P3HT (Sepiolid P200, BASF) and 60PCBM (99%, Solenne B.V.) solutions that were respectively 50, 30, and 15 mg mL^{-1} and 40, 30, and 15 mg mL^{-1}. The substrate was prepared starting from PET foil with a width of 305 mm fully covered by ITO (60 Ω $square^{-1}$) by screen printing a UV-curable etch resist, followed by etching ($CuCl_2$), stripping, washing, and drying as described earlier. The PET-ITO substrate comprised 16 parallel stripes of ITO (13 mm wide separated by 2 mm) with a length of 225 mm and a repetition length of 250 mm. Cleaning of the PET-ITO substrate on both sides using isopropanol was carried out prior to coating. Each solar cell was labeled on the backside using an inkjet printer. The aluminum doped zinc oxide layer was prepared by slot die coating a methanol solution prepared as follows. $Zn(OAc)_2 \cdot 2H_2O$ (100 mg mL^{-1}) and $Al(O)(OAc)_2$ (basic) (1.5 mg mL^{-1}) were stirred by heating to 50 °C for 1 h and left to cool for 24 h, whereby some material precipitates. The solution was filtered (0.45 μm filter) and used directly for coating. The PEDOT:PSS (EL-P 5010, Agfa) was adjusted to a viscosity of 270 mPa s using isopropanol. The silver inks for the back electrodes were used without further modification. Heat curing PV410 (Dupont) was used for grid electrodes and UV-curing Toyo Ink was used for the full electrodes. A barrier material (Amcor) with an adhesive (467 MPF, 3M) was employed for encapsulating the devices.

Roll-to-Roll Equipment. The roll-to-roll coating machine employed for slot-die coating in this study was comprised of an unwinder, corona treater, double-sided web cleaning unit (TekNek) antistatic bars, coating roller, hot air oven, cooling roller, and rewinder. The oven was operated at 140 °C during drying of all layers. The roll-to-roll flat bed screen printer employed in this study comprised an unwinder, position and registration unit, vacuum table, printing unit, hot air oven, UV-curing station, transport roller, dancing tensioning roller, and rewinder. The laminator comprised an unwinder, edge guide, splicing table, lamination rollers, unwinder for the overlaminating foil, and rewinder for the laminated material.

Slot-Die Coating Head, Pumping, and Mixing. A standard slot-die coating head with a working width of 250 mm and a dead volume of 50 mL in the feed manifold was employed for coating of the zinc oxide layer and the PEDOT:PSS layer. The ZnO layer was applied by use of a piston pump (Knauer) with a pumping capacity of up to 50 mL min^{-1} in steps of 10 μL. The PEDOT:PSS was applied using a static pressure tank for feeding the ink. The custom-made mini slot-die coating head had a single slot 13 mm wide, 40 mm long and 0.05 mm thick giving a dead volume of 26 μL. The single slot coating head was fed by 1/16 in. tubing with an internal diameter of 0.1 mm and a length of 800 mm giving a nominal dead volume of 6.2 μL. The two pumps (Knauer) had a maximum pumping capacity of 10 mL min^{-1} in steps of 1 μL. The exit from each pump was fed into a mixing-T (UP-U428, Upchurch) with a nominal dead volume of 2.8 μL. The total dead volume from the mixing-T through the wire and the mini slot-die coating head to the substrate was approximately 35 μL. The nominal volume required for one solar cell repeat with a wet thickness of 9.6 μm is 10.3 μL.

Coating and Printing of the Layers. The zinc oxide layer was coated on all stripes simultaneously using the standard slot-die coating head. The web speed was 2 m min^{-1} and the ink was supplied to the coating head at a rate of 2 mL min^{-1} giving a wet layer thickness 4.8 μm. The dried ZnO layer was cured for 10 min at 140 °C. The active layer was then coated in single stripes as described above. The PEDOT:PSS was applied using the standard slot-die coating head while coating only the 6 of the stripes where experiments were made. In principle all 16 stripes could be employed but it was found most practical to have some spacing between experiments and thus a practical choice of 6 experiments per roll width was made. Finally a silver back electrode was applied onto the substrate that was either fully covering or a grid structure with a 20% area coverage using screen printing.

Characterization. The roll with the 6 stripes each comprising an experiment with 200 cells (i.e., a total of 1200 solar cells) was mounted in a roll-to-roll solar cell characterization machine and the cells were forwarded to the measuring position controlled by a register mark applied during printing of the silver back electrode. The solar simulator was calibrated for AM1.5G (1000 W m^{-2}). The devices were masked such that only the active area was illuminated during measurements. Electrical contact was made using pneumatic cylinders and the IV-curves for the cell in question were recorded using a Keithley 2400 sourcemeter. After measurement the contact was broken and the foil forwarded until the next cell was in position. Typical measuring time for each cell was 20 s allowing for the collection of 3 IV curves. The transport and positioning time took 15 s. The data was saved in several file formats for later analysis. The thickness was obtained by delaminating at the interface between the active layer and the PEDOT:PSS layer. The optical density was recorded for all cells and AFM was used to determine the thickness for every 10 cells. This gave an accurate determination of the variation in thickness along the roll.

Statistical Analysis. A total of ca. 9000 individual solar cells were prepared and studied in this report. For the studies on the P3HT:PCBM ratio the step size was 0.5−1% and thus 100−200 individual cells covered the entire phase diagram. For each 100 or 200 cell experiment, an extra 25−50 solar cells are prepared before and after the actual experiment. The thickness experiment also employed a 0.5−1% step size with a total of 100−200 cells being prepared. The two types of experiments were each carried out 24 independent times using step sizes of both 0.5 and 1%.

RESULTS AND DISCUSSION

Considerations of Sampling Method and Speed.

The use of point sampling to map a parameter space is

critically influenced by the speed of sampling and in the case of polymer solar cells where each laboratory sample is typically represented by a glass substrate we estimate that the investment in time per sample is on the order of 1 h (based on a batch of 10−12 glass substrates and evaporated electrodes) and requires about 10−20 mg of donor/acceptor mixture. Assuming that one aims at exploring two processing dimensions such as donor/acceptor ratio and active layer thickness with some accuracy 10 samples would be required in each dimension and if the ratio-thickness surface is to be sampled with the same accuracy, a total of 100 samples would be needed. Depending on the availability of material it is clear that the careful investigation of just these two parameters would require gram quantities of material and possibly 1−2 weeks of investigator time. Adding other processing dimensions such as additives, thermal annealing, and solvent annealing would evidently increase the complexity and work correspondingly. It is not straightforward to devise a novel approach that removes the dependence on rigid substrates comprising indium−tin-oxide-coated glass substrates and spin-coating for film formation while at the same time increasing both speed and efficiency of sampling. When having set this goal, one can pursue an approach that involves improvement of the efficiency with which the traditional route is followed. This was excellently demonstrated by Riede et al. (9) in an experiment that employed an automated setup for the measurement and handling of the final substrates while the individual substrates were still prepared and handled by hand. An entirely different methodology would be to employ an endless substrate material and vary the processing dimension along the length of the material. One method that inherently gives access to such a sampling scheme is roll-to-roll coating. This has the additional advantage of being able to produce polymer solar cells that are very close to the intended final form. One is thus able to skip the step of going from individual glass substrates to a manufacturing setting later on, which should be considered a large advantage.

Considerations of Roll-to-Roll Coating and Characterization. Several film forming methods exist when using roll-to-roll coating such as gravure, flexographic, screen, slot-die printing, and coating. All methods have been attempted to be used in the context of polymer solar cells while a combination of slot-die coating and screen-printing has been the most successful in the context of inverted devices (11), where it was shown that normal and inverted devices with evaporated electrodes gave the same performance. The inverted device structure employs a solution-processed zinc oxide layer as the electron contact (12). Common to all methods is that they fall very short of fulfilling the requirement for parsimony in materials use. In Figure 2, the differences between the commonly employed spin-coating technique and the slot-die-coating techniques has been illustrated. The main difference between the two techniques is that the spin coating technique operates on a discrete substrate whereas the slot-die coating technique operates on a continuous roll of material. This brings in the possibility for variation in the film composition in time (and along the length of the roll). This is explored in this work. Most techniques easily require in excess of 100−1000 mL of solution or printing ink before they are operational. Recently, a modified slot-die coating procedure was demonstrated to enable the successful coating of polymer solar cells while the ink consumption was reduced significantly to 5−10 mL (13). This typically allowed for the preparation of many devices but did not enable the controlled variation of parameters such that process dimensions could be explored (essentially representing point sampling). For traditional slot-die coating, the dead volume in the coating head is what prevents the exploration of processing dimensions vis-à-vis the discussion above. By making an additional modification to slot-die coating such that the dead volume is reduced and adding the coating solution differentially pumped, it becomes possible to vary the composition of two (or more) materials in the coated film as it passes the coating head by varying the rate at which components are fed to the slot-die coating head. The reason for the large dead volume in traditional slot-die coating is that the method is used for coating large areas evenly or for the formation of stripes of solar cell material comprising individual solar cells that can be serially connected at a later stage. This requires a feed manifold that yields a constant and even flow of liquid ink over the entire breadth of the slot-die coating head and hence some volume is required. By reducing the breadth of the coated area to 1−2 cm it is possible to reduce the effective dead volume to much less than 100 μL, and this modification is what has enabled our use of slot-die coating in reaching the goals stated above. The typical web speed employed in these experiments was 2 m min^{-1} and the coating width was 13 mm wide areas. Up to four stripes were successfully coated simultaneously in this manner, but it was found beneficial to coat one single 13 mm wide stripe at a time as the flow was most easily controlled and the materials usage was reduced to a minimum.

The procedure typically yielded an enormous amount of solar cells (750−1500 in one run) and in order to be efficient the characterization of the solar cells also has to be fast and efficient. Because the material is on a roll of material the simplest method was found to be the use of a solar simulator comprising an automated positioning and contacting system such that the solar cells could be both prepared and characterized by a roll-to-roll process (3). To compare the speed and sampling efficiency of the traditional laboratory approach employing rigid glass substrates and point sampling with our roll-to-roll processing method one can examine the sampling quality, speed, and materials usage. In the typical laboratory experiment the characterization of a processing dimension such as donor−acceptor ratio using 10 sampling points would require 100 mg of material and would require ∼60 min of laboratory work per sample. It would enable reasonable accuracy in the determination of the optimum donor−acceptor ratio. With our method, 200 sampling points would be prepared using 60 mg of material and requiring a total of 35 s per sample. This represents an

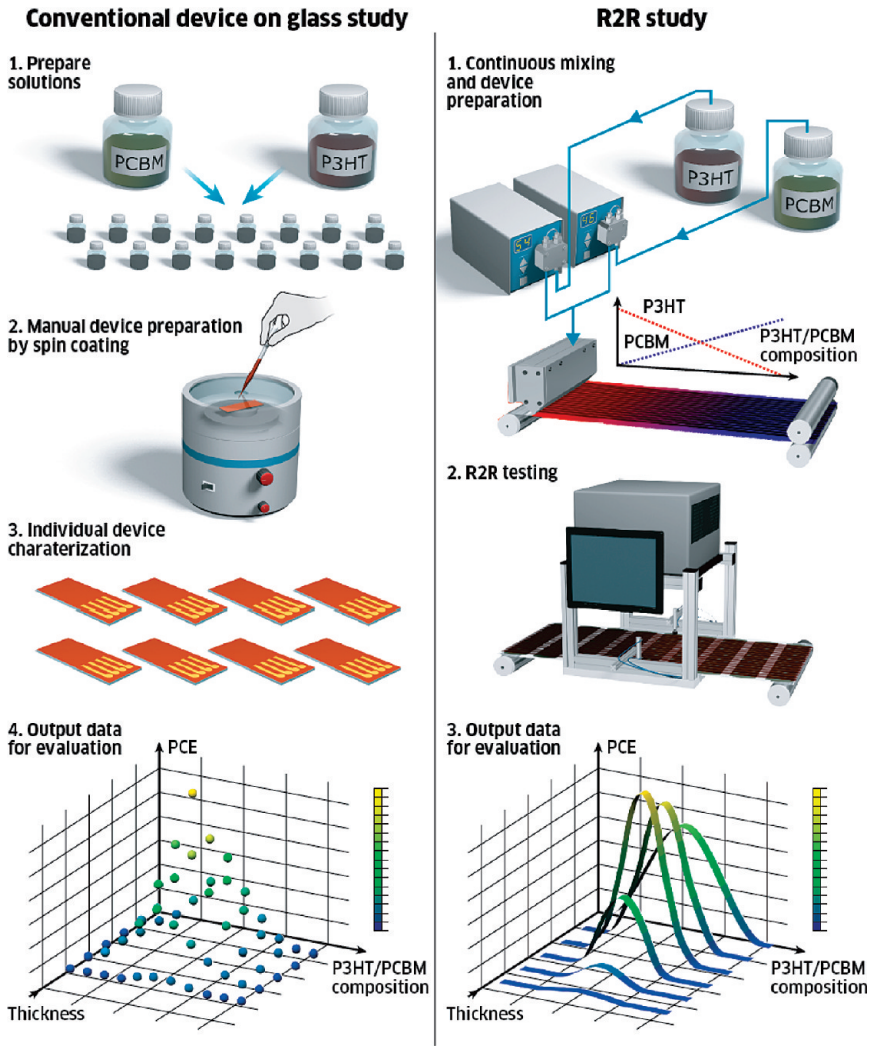

FIGURE 2. Comparison between preparation and characterization of conventional polymer solar cells on glass (left) and those prepared in this work using roll-to-roll methods (right). Variation of, for example, the active layer composition typically requires the preparation of many solutions with different composition (from stock solutions). These solutions are then spin-coated onto individual substrate slides and processed into devices. In the R2R process, two stock solutions are differentially pumped into a slot-die coating head and coated onto a plastic roll in a continuous stripe, giving 12 devices per meter. The devices are the automatically measured on a roll-to-roll characterization machine to give data covering the whole range of compositions in small steps.

increase in speed by a factor of 100, an increase in the accuracy by a factor of 20, and an increase in the efficiency of materials usage by a factor of 2. In this case, a net improvement by several orders of magnitude (~4000 times) is possible when considering just these three factors. Other advantages such as closeness of the approach to the final form of the solar cell etc. would count toward the quality of this approach. Figure 2 illustrates the sampling of the parameter space and the roll-to-roll methodology.

Donor–Acceptor Ratio. When exploring the donor–acceptor ratio in the traditional laboratory experiment, many discrete solutions must be procured by carefully weighing or dispensing the donor and acceptor material in the required amounts. In the roll-to-roll method described here, separate stock solutions of donor and acceptor material in the desired solvent is pumped via separate paths into a mixing head. This has the advantage that the donor and acceptor material is not mixed until it is to be used and one can, for instance, employ the same stock solution of donor material with different acceptor materials by simply changing the source solution for the pump. In the P3HT-PCBM case where the optimum is around a 1:1 mixture this implies that the concentration of the components in the stock solution has to be twice as high as the concentration at which they are applied to the substrate. In a typical experiment 30 mg mL^{-1} stock solutions of P3HT and PCBM were pumped through the mixing head to the slot-die coating head and the composition applied to the substrate. The typical flow rate was 0.25 mL min^{-1} and the web speed was 2 m min^{-1}. The delay is given by the dead volume in the feed hose from the mixing head to the slot-die coating head and the dead volume in the slot-die coating head. The nominal dead volume was 35 μL which is the ~3 times the typical amount required to prepare one device (13 mm wide, 83.3 mm long). The practical dead volume is somewhat higher because of the inhomogeneous flow in the feed hoses and connections and mixing of the components in the meniscus between the slot-die coating head and the substrate. We determined the effective dead volume to be 6 solar cells due to inhomogeneous flow and 2–3 solar cells due to the

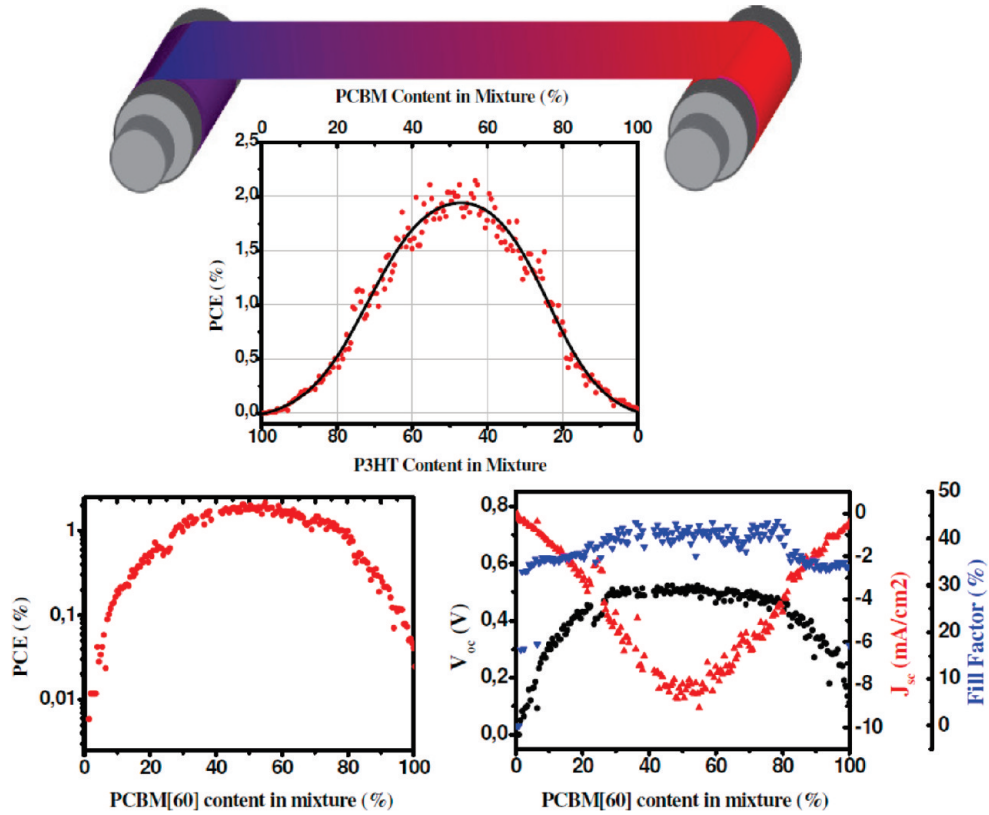

FIGURE 3. Variation in device performance as the composition of the P3HT-PCBM mixture is varied. The compositional step size in this experiment was 0.5% and the result was independent of whether the experiment started with PCBM or P3HT devices (above). When plotting the power conversion efficiency on a logarithmic scale it is noted that the performance of pure P3HT devices are lower than pure PCBM devices by approximately a factor of 10 (lower left). The variation in performance over the compositional range is mainly due to changes in current as voltage and fill factor are nearly constant over the compositional range. Data for 200 devices are shown.

standing meniscus. The experiment started with pumping 100% P3HT (0.25 mL min^{-1}) and 0% PCBM (0 mL min^{-1}) solutions. The flow from the pumps was thus changed in steps of 0.5−1% by decreasing the P3HT flow and increasing the PCBM flow. The distance in time between steps was typically triggered by the passage of a new cell under the slot-die coating head. This could be varied at will as could the order of pumping the solutions. The minimum pumping step size was 1 μL min^{-1}. The total flow to the coating head was kept constant and the wet layer thickness is thus constant throughout the experiment ($\sim$ 9.6 μm).

The variation in dry layer thickness is given by the differences in density for the two components. The experimental result is shown in Figure 3 where it is seen that the optimum performance is reached in a relatively broad range of composition. At 100% P3HT poor performance is observed (PCE $\sim$0.006%) and at 100% PCBM a slightly better performance is observed (PCE $\sim$0.05%). Both those solar cell types correspond to single-layer solar cells. In between those two points bulk heterojunction type devices are formed with an optimum ratio at around 50% P3HT and 50% PCBM as shown in Figure 3. Representations of the photovoltaic parameters as a function of composition for P3HT:PCBM have been reported earlier but only a few cases document optimum parameters significantly removed from the optimum composition (14). Our results confirms earlier findings albeit in much greater detail and with precision throughout the entire composition space. Recent work (15) has demonstrated an optimal composition that is far removed from the typical 1:1 mixing ratio. Interestingly, a mixing ratio of 1:1 in that case performed relatively poorly and the performance increased tremendously only when extreme mixing ratios of approximately 1:10 were reached. This implies that the commonly explored materials screening would fail to identify potential high-performance materials as the extreme mixing ratios are normally not explored. We would expect the method presented here to more efficiently identify new polymer materials that exhibit this behavior.

Optimum Thickness. In addition to the optimization of the donor−acceptor ratio it is also of interest to find the optimum thickness for the active layer. Ideally one should strive for as thin a layer as possible that gives the required absorption and performance. However, as the film thickness decreases other factors come into play such as pin-holes and defects that may ultimately yield dysfunctional devices. The determination of the optimal thickness is again efficiently sampled by diluting the mixture of donor and acceptor with solvent during coating thus keeping the wet layer thickness constant while decreasing the concentration of the active materials and therefore the dry layer thickness. The experiment was carried out starting with the active components with gradual dilution to infinity or conversely by starting with pure solvent while gradually increasing the concentration of the active materials to full concentration. The results are shown in Figure 4. As expected the performance drops to

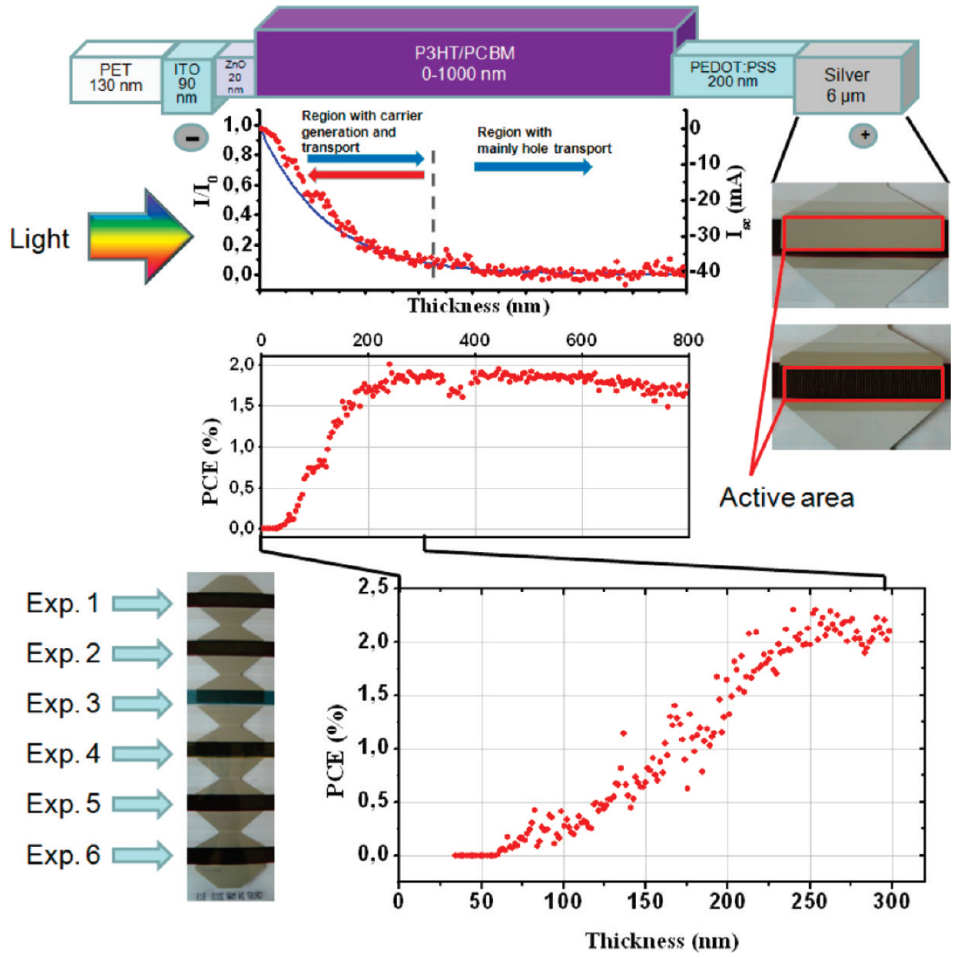

FIGURE 4. Thickness variation for P3HT-PCBM solar cells with a layer sequence as outlined schematically (top).The performance of the device is shown as a function of varying the active layer thickness while keeping all other parameters constant. Illumination leads to absorption (blue curve) and carrier generation in the first 300 nm of the film thickness and carrier transport only in the remaining part of the film thickness (upper plots). Very thick films were studied with thickness steps of 4 nm (middle plot) and thinner films with thickness steps of 1.5 nm were also studied (lower plot). One module from the role showing 6 independent experiments is shown from the front side (lower left) along with the two different printed silver electrode patterns (fully covering and grid electrodes) having the active area highlighted by a red rectangle (upper right).

zero as the films get very thin giving no absorption and short circuits. At a thickness of around 50 nm the coated film is fully covering and functional devices can be consistently prepared using this method. An interesting point to observe is that the voltage quickly stabilizes at the value of the open circuit voltage (V_{oc}) while current gradually increase due to increased absorption (see Supporting Information, Figure S1). Intuitively one would expect the current to drop as the film became thicker and therefore a narrow maximum in the power conversion efficiency as a function of thickness was expected. Yet, for the thickness ranges explored here that gives functional devices (50−800 nm) the power conversion efficiency increase throughout the thickness range explored (0−800 nm) with the most rapid increase at the lower thicknesses (<150 nm). This is of practical significance as variations in thickness will not lead to significant changes in performance. In terms of processing polymer solar cell devices it implies that one should strive for layer thicknesses of around 150 nm to minimize the materials usage while guaranteeing good performance (see Supporting Information, Figure S1).

Optical Effects. It was anticipated that optical interference effects (as an example see Figure 1 in ref 1) would be observable because of variation of the active layer thickness as is commonly observed for devices employing multilayers and reflective back electrodes (16).

In this work, where either semitransparent or nontransparent printed back electrodes were employed the influence of optical interference effects on the performance of the devices was not observed. In an experiment such as the one we present here with many data points and many devices with small increments in active layer thickness (1.5−4 nm increments), it was expected that the optical effects would be observed if present. This finding has some consequence for the arguments for employing optical spacers to improve performance. From a fundamental point of view, optical inference effects are present in multilayer structures where the layers have different refractive indices and the interfaces are sharp. The fact that we do not observe any optical interference effects has the important implication that it is not necessary to take the thickness of the active layer into account in the context of roll-to-roll coated polymer solar

cells of this type as long as the thickness ≥150 nm. At a thickness above 150 nm, the voltage is consistent and the absorption is large enough for any optical interference effects to be negligible. An explanation for the absence of optical interference effects observable as oscillatory variations in device performance with active layer thickness may in part be due to a significant roughness at the interfaces such that they do not appear optically discrete to the incoming light. The roughness for the various interfaces are for ITO, ZnO, P3HT-PCBM, and PEDOT:PSS, respectively, 1.7, 3.39, 14.6, and 106 nm. On the basis of this, optical interference should be observable and we sought the explanation through the light source. The AM1.5G standard represents the solar spectrum and includes a significant diffuse component (10%). Because of this, it is likely that the optical interference effects are present but not observable under illumination with white light, which would also smooth the optical interference effects in the entire wavelength region where the active layer exhibit conversion of light into an electrical current. To investigate this further, we thus recorded IPCE spectra for all thicknesses from 0−800 nm active layer thickness in steps of 4 nm and found no observable variation in the IPCE as a function of layer thickness that could be ascribed to optical interference (see supplementary data). Although we cannot exclude the presence of optical interference effects, we conclude that it is only weakly (if at all) influential on the performance of the solar cell type presented here. Further, the semitransparent nature of the devices with the lack of a reflective back electrode limits the optical interference effects to the components of light reflected due to differences in refractive index between the different layers at the interfaces of the active layer-PEDOT:PSS and the PEDOT:PSS-adhesive interface at the back electrode. Because the differences in refractive indices are small, it can thus be anticipated that the effect is small. Finally, it is clear from Figure 4 that once most of the light has been absorbed (after ∼300 nm) the efficiency remains constant. The material at a thickness greater than 300 nm thus serves only as a carrier transport layer and because the losses are small, very thick devices work well. In terms of materials usage, it is of course desirable to employ layers with a thickness sufficient to achieve good performance but not so thick that the material does not contribute toward increased performance. On this basis, it would also seem that any attempts to employ optical spacers for this type of device geometry is futile.

Doping of the Electron Transport Layer. One commonly observed electrical phenomenon when employing oxide based semiconductors as carrier transport layers in polymer solar cells is the appearance of an inflection point (S-shape) in the IV curve due to accumulation of charges at one of the interfaces (17). In the case of the device type explored here, the electron transport layer is zinc oxide, which is known to exhibit a significant dependence of the electron transport on the oxygen doping level. Illumination with UV light or the application of a large electrical bias can reverse the effect (18) and remove the inflection point until the device is left in the dark where it gradually reappears (3). The time it takes to anneal out the inflection behavior is normally 10−30 min under full illumination (AM1.5G, 1000 W m^{-2}). In the context of this work, where we sought a fast method, it was found highly impractical that every device would need on the order of half an hour of annealing time. It has been discussed earlier in the context of upscaling this technology that the extra time the annealing takes can make a significant impact on the cost structure and annual production (3). A typical experiment as we describe here employing 200 solar cells would thus require 100 h of charaterisation time which clearly represents a bottleneck that would make the very high efficiency of all the other steps presented less useful. We thus needed a strategy to remove the inflection point and explored the use of aluminum doping of the zinc oxide. Aluminum doping is a well-known approach to increase the conductivity of zinc oxide (19) and from this point of view the approach was trivial. The challenge was, however, to make a roll-to-roll compatible process. We found that coating a mixture of zinc acetate and aluminum acetate from methanol solution efficiently addressed this point and gave inflection free devices after curing at a temperature of 140 °C. When using aluminum doped zinc oxide the fill factors decreased slightly and the device was not as hole blocking at reverse bias. Yet performance was independent of illumination time and the characterization of one solar cell on the roll-to-roll characterizer typically took 35 s including the time for transporting the foil, positioning the cell and making the electrical contacts. In this fully automated process, an experiment with 200 cells could typically be fully characterized in an hour.

The complexity of the makeup of polymer solar cells brings along with it the challenge of efficiently characterizing a particular materials combination in a given device geometry. In spite of intense research on popular materials combinations such as P3HT:PCBM it is therefore likely that the parameter space is not yet fully explored. The scientific community still discovers new aspects of processing this well-known system. From this point of view it is clear that the previously available techniques do not efficiently enable fast mapping of the parameter space for a given material. We describe here a method for fast and efficient mapping of variation in photovoltaic performance parameters as a function of materials composition and layer thickness. In our demonstrations, the method was applied to the active layer, but could easily be applied to other layers in the solar cell stack or modified to include variation of more components and additives. The increase in the speed of solar cell preparation and characterization by orders of magnitude compared to conventional laboratory techniques opens up a range of possibilities enabling the experimenter to focus on more detail while having a significant statistical basis for making conclusions. The massive number of observations also has the advantage that outliers are easily spotted and conclusions can be made on the basis of the average rather than single observations.

The method has demonstrated several unexpected points related to the layer thickness. First, no optical interference effects were observed as a function of layer thickness under illumination with white light (AM1.5G). We further examined this by using a series of monochromatic light sources in the range of wavelengths where the P3HT:PCBM mixture exhibits a significant photoresponse (390−690 nm) and observed the same behavior as under illumination with white light. Second, we found that the performance was quite constant with layer thickness in the range of 300−800 nm and estimate that very thick films (4000−5000 nm should yield functional polymer solar cells based on P3HT:PCBM. The performance was nearly constant at thicknesses above 300 nm, where the slight increase in current due to increased optical absorption was balanced by a slight decrease in fill factor thus yielding nearly constant power conversion efficiency (see the Supporting Information). Although it was of interest to prepare films with thicknesses larger than 800 nm, this was practically limited by the solubility of the components in chlorobenzene. The thickest films we could make were based on solutions that were 40 mg mL^{-1} with respect to PCBM and 50 mg mL^{-1} with respect to P3HT. This solution has a solid content of nearly 10%, which is exceptionally high. Thicker films would require solid contents close to 50%, which is not possible with available solvents.

CONCLUSIONS

The new method we present enables very fast and complete processing and characterization of thousands of roll-to-roll processed polymer solar cells with less than 100 mg of material, which would be impossible using conventional methods. Approximately 10 μL of solution is used for the preparation of each solar cell without any loss of material. The method enables a very detailed investigation of the influence a given parameter may have on for instance the performance of the polymer solar cell. We demonstrated this for both the composition of the active layer and for the thickness of the active layer. The principle is concluded to be general and extendable to other processing dimensions such as additives, dopants, and surface treatments. We expect this method to prove very useful for the screening of new materials, where limited quantities are available.

Acknowledgment. We thank Kristian Larsen and Torben Kjær for technical assistance. Thomas Tromholt is thanked for making the AFM measurements. This work was supported by the Danish Strategic Research Council (DSF 2104-05-0052 and 2104-07-0022) and EUDP (j. nr. 64009-0050). A patent application covering the inventions described in this article has been filed.

Supporting Information Available: Details of IPCE measurements as a function of active layer thickness, variation of all photovoltaic parameters as a function of thickness, thickness plot, absorption spectra and AFM images, typical IV curves, and photographs of the experimental setup and coating experiments (PDF). This material is available free of charge via the Internet at http://pubs.acs.org.

REFERENCES AND NOTES

(1) Dennler, G.; Scharber, M. C.; Brabec, C. J. *Adv. Mater.* **2009**, *21*, 1323–1338.
(2) Krebs, F. C. *Sol. Energy Mater. Sol. Cells* **2009**, *93*, 394–412.
(3) Krebs, F. C.; Tromholt, T.; Jørgensen, M. *Nanoscale* **2010**, 1; published online http://dx.doi.org/10.1039/b9nr00430k.
(4) Ma, W.; Yang, C.; Gong, X.; Lee, K.; Heeger, A. J. *Adv. Mater.* **2005**, *15*, 1617–1622.
(5) Li, G.; Shrotriya, V.; Huang, J.; Yao, Y.; Moriarty, T.; Emery, K.; Yang, Y. *Nat. Mater.* **2005**, *4*, 864–868.
(6) Peet, J.; Kim, J. Y.; Coates, N. E.; Ma, W. L.; Moses, D.; Heeger, A. J.; Bazan, G. *Nat. Mater.* **2007**, *6*, 497–500.
(7) Lee, J. K.; Ma, W. L.; Brabec, C. J.; Yuen, J.; Moon, J. S.; Kim, J. Y.; Lee, K.; Bazan, G. C.; Heeger, A. J. *J. Am. Chem. Soc.* **2008**, *130*, 3619–3623.
(8) See www.solarmer.com.
(9) Riede, M. K.; Sylvester-Hvid, K. O.; Glatthaar, M.; Keegan, N.; Ziegler, T.; Zimmermann, B.; Niggemann, M.; Liehr, A. W.; Willeke, G.; Gombert, A. *Prog. Photovolt: Res. Appl.* **2008**, *16*, 561–576.
(10) Tromholt, T.; Gevorgyan, S. A.; Jørgensen, M.; Krebs, F. C.; Sylvester-Hvid, K. O. *ACS Appl. Mater. Interfaces* **2009**, *1*, 2768–2777.
(11) Krebs, F. C.; Gevorgyan, S. A.; Alstrup, J. *J. Mater. Chem.* **2009**, *19*, 5442–5451.
(12) Beek, W. J. E.; Wienk, M. M.; Kemerink, M.; Yang, X.; Janssen, R. A. J. *J. Phys. Chem. B* **2005**, *109*, 9505–9516.
(13) Krebs, F. C. *Sol. Energy Mater. Sol. Cells* **2009**, *93*, 465–475.
(14) Müller, C.; Ferenczi, T. A. M.; Campoy-Quiles, M.; Frost, J. M.; Bradley, D. D. C.; Smith, P.; Stingelin-Stutzmann, N.; Nelson, J. *Adv. Mater.* **2008**, *20*, 3510–3515.
(15) Subbiah, J.; Beaujuge, P. M.; Choudhury, K. R.; Ellinger, S.; Reynolds, J. R.; So, F. *ACS Appl. Mater. Interfaces* **2009**, *1*, 1154–1158.
(16) Schueppel, R.; Timmreck, R.; Allinger, N.; Mueller, T.; Furno, M.; Uhrich, C.; Leo, K.; Riede, M. *J. Appl. Phys.* **2010**, *107*, 044503.
(17) Glatthaar, J.; Riede, M.; Keegan, N.; Sylvester-Hvid, K.; Zimmermann, B.; Niggemann, M.; Hinsch, A.; Gombert, A. *Sol. Energy Mater. Sol. Cells* **2007**, *91*, 390–393.
(18) Verbakel, F.; Meskers, S. C. J.; Janssen, R. A. J. *J. Appl. Phys.* **2007**, *102*, 083701.
(19) Minami, T.; Nanto, H.; Takata, S. *Jap. J. Appl. Phys.* **1984**, *23*, L280–L282.

AM100505E